# Effect of Thermally Expanding Surfaces on Aerodynamic Roll Torques for Cones

JOHN B. MCDEVITT*
*NASA Ames Research Center, Moffett Field, Calif.*

**An experimental and analytical study has been made of the aerodynamic roll torque on smoothly ablating, spinning cones. The tests, conducted in the Ames 3.5-Foot Hypersonic Wind Tunnel, indicated that the smoothly ablating model rolling at 0° angle of attack experiences roll damping, but when rolling at angle of attack an aerodynamic torque in the direction of spin arises if thermal expansion of the body surface occurs. An analysis of the spinning body at angle of attack is included to show how the relative importance of the ablator thermal expansion and the surface recession rate determines whether the motion is damped or undamped.**

## Nomenclature

$A_b, d$ = model base area and diam
$C_l$ = rolling moment coefficient, $L/q_\infty A_b d$
$C'_{l_f}$ = slope of aerodynamic friction moment coefficient
$C_N$ = normal force coefficient, $N/q_\infty A_b$
$C_{N_\alpha}$ = normal force coefficient slope
$C_p$ = pressure coefficient
$h, h_0, h_\alpha$ = heating rate parameters, Eq. (1)
$K_\varepsilon$ = see Eq. (2)
$K_1, K_2$ = see Eq. (5)
$\bar{K}_1, \bar{K}_2$ = see Eq. (7)
$L$ = rolling moment
$l$ = cone length
$M_\infty$ = freestream Mach number
$m, n, \bar{n}$ = exponents, Eqs. (1 and 3–5)
$N$ = normal force
$p, \dot{p}$ = roll rate, rad/sec, and roll acceleration, rad/sec$^2$
$P_{t_1}$ = total pressure
$q_\infty$ = freestream dynamic pressure
$r$ = cone radius
$R$ = cone radius during ablation
$\Delta r$ = mean changes in cone radius, Eq. (5)
$t$ = test time, sec
$U_e$ = stream velocity at edge of cone boundary layer
$W$ = model weight
$x$ = axial coordinate
$\bar{y}$ = lateral movement in c.g.
$y, z, \theta$ = spatial coordinate system, Fig. 8
$\alpha, \beta$ = angles of attack and sideslip
$\sigma_c$ = cone semivertex angle
$\varepsilon$ = azimuthal angle at minimum boundary-layer displacement thickness, Fig. 8
$\lambda$ = see Eqs. (3) and (4)
$(\ )_b$ = at model base
$(\ \cdot)_1$ = arising from ablation mass removal, Eq. (5)
$(\ )_2$ = arising from thermal expansion, Eq. (5)

## Introduction

ANOMALIES in the flight behavior of various slender entry vehicles have prompted numerous studies of the interaction between the gaseous products of ablating heat shields and the hypersonic stream, of the effects due to shape changes arising during ablation, and of possible coupling between ablation pattern development and aerodynamic roll torque. With regard to the latter phenomenon two recent papers[1,2] describe wind-tunnel measurements of aerodynamic torque on conical ablating models. In Ref. 1 a conventional strain gage balance was used to measure static rolling moments while in Ref. 2 a gas bearing was employed that allowed the test models to be free in roll, and thus the dynamic aspects could be included in the study. Both subliming and melting-vaporizing ablators were used. The effects of various pattern developments (streamwise vortex grooving, turbulent wedge erosion, and cross-hatching) on roll torque were noted. However, a surprising behavior was observed in Ref. 2 for one of the melting-vaporizing test models—the immediate spin up of a smoothly ablating model when prespun and inserted into the test stream at angle of attack. Although the result was unexpected at the time, a simple explanation may be offered on the basis of the thermal expansion characteristics of the ablating material and the effect of spin at angle of attack on local heating rates. A study of this new phenomenon, whereby aerodynamic torque for rolling models at angle of attack can arise through the thermal expansion characteristics of the ablator, is described in this paper.

## Facility, Models, and Apparatus

The tests were conducted in the Ames 3.5-Foot Hypersonic Wind Tunnel at $M_\infty = 7.4$, $P_{t_1} = 102$ atm, and at a nominal total temperature of 1100°K resulting in a nominal freestream Reynolds number of $1.4 \times 10^6$/m ($4.5 \times 10^6$/ft). A quick-insert, model-support mechanism permits insertion of the model into the test section after the tunnel reaches preselected, steady-state stream conditions, and retraction when data acquisition has been completed.

Two test model designs (designs A and B of Fig. 1), differing only in the diameter of the cylindrical afterbody, were considered because of concern that products of ablation might collect on the

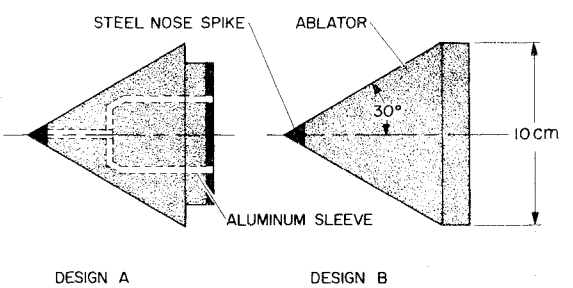


**Fig. 1 Test models.**

Presented as Paper 72-30 at the AIAA 10th Aerospace Sciences Meeting, San Diego, Calif., January 17–19, 1972; submitted January 26, 1972; revision received November 10, 1972.

Index categories: Entry Vehicle Dynamics and Control; Nonsteady Aerodynamics; Material Ablation.

* Research Scientist. Associate Fellow AIAA.

afterbody or base and affect the roll measurements. However, experience with ablating models indicated that the afterbody design did not noticeably affect the results. For the present study one all-metal nonablating (design A) model and eight ablating models (one of design A, the remainder of design B) were constructed. The ablation material used was "special Korotherm" (see discussion by Williams[1] of this relatively low-temperature ablation material) that was cast about the aluminum sleeve.

The one-degree-of-freedom (roll) gas bearing on which the models were mounted is described in detail in Ref. 2. A photodiode device was used to record the roll rate of the model. Two air lines, directed obliquely towards the model base, provided a means of prespinning the model in either direction.

## Results and Discussion

Since the primary purpose of this study was to determine the influence of smoothly ablating surfaces (no surface patterns of any kind) on aerodynamic roll torques, the behavior of the Korotherm ablator in the present test environment will be discussed in some detail before presenting the roll test results.

### Korotherm Surface Behavior under Heating

In the present test environment, the Korotherm material appeared to ablate in a melting-vaporizing fashion with part of the mass loss through liquid-layer runoff but most of the mass loss through vaporization. Motion pictures of the ablating models show that a thin liquid layer appears within a few seconds after the model is inserted into the stream and flows rearward, interacting momentarily with the supersonic flow to form moving oblique wave patterns. The latter phenomenon, studied in detail by Nachtsheim,[3,4] persists for only a second or so and disappears as the melt layer thickens. This transient, liquid-layer wave pattern is not believed to contribute to the aerodynamic roll torques discussed in this paper.

The motion pictures also showed that, except for the transient wave pattern early in the test run and an occasional indentation caused by impingement of a dust particle in the stream, the melting-vaporizing surface remained remarkably smooth for the test times up to about 20 sec. An important contributing factor here is believed to be the relatively large thermal expansion of Korotherm material that effectively delayed the formation of a rearward-facing step at the base of the metal tip [a fortunate situation, indeed, since rearward facing steps are known to cause longitudinal grooves and turbulent wedge patterns in ablating surfaces (e.g., Ref. 2)]. After about 20 sec of testing, however, the ablating surfaces no longer remain smooth, and the motion pictures show the formation of streamwise vortex grooves, emanating from the base of the metal tip, followed by the rapid formation of turbulent wedge regions and eventually cross-hatching. The effect of ablation striations on roll torques was studied in Ref. 2 and since the intent of the present investigation was to study smoothly ablating cones with large thermal expansion characteristics the present tests were limited to test times of about 17 sec, which, in effect, confined the experiments to the smoothly ablating case.

### Tests at $\alpha, \beta = 0$

The aerodynamic roll behavior of a Korotherm cone and a nonablating metal cone are presented in Fig. 2. The models were prespun to about 10 rad/sec and inserted into the test stream at zero angle of attack ($\alpha$) and zero sideslip ($\beta$). The time required to insert the model into the test stream was set at $\frac{1}{2}$ sec for the present tests and the test time $t$ was measured from the instant the model reached the inserted position (tunnel centerline). The indication of small, positive $\dot{p}$ values before $t = 0$ is a reflection of the internal torque in the gas bearing (see discussion in Ref. 2). In both cases the model-rotor assembly has approximately the same inertia about the roll axis. A tare value of $\dot{p}/p = 0.004$ should be subtracted to obtain the aerodynamic damping, as illustrated by the dashed curve shown for the nonablating model in Fig. 2.

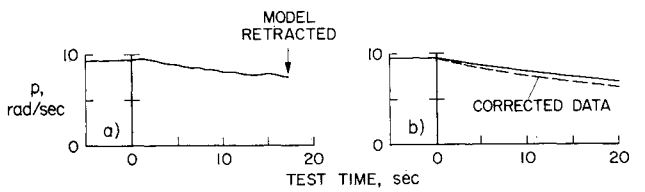


**Fig. 2 Roll characteristics at $\alpha, \beta = 0°$; a) ablating model, b) nonablating model.**

For the ablating model the roll history is not the smooth variation with time evidenced by the nonablating model, although the mean aerodynamic damping is approximately the same. The slight irregularities in the motion of the ablating model are believed to arise from mass asymmetries introduced when the model traverses the varying heating environment of the tunnel boundary layer or from nonuniform thermal properties of the Korotherm material. In any event, the roll motion is damped at about the same rate exhibited by the nonablating model.

### Tests at $\alpha, \beta = \pm 5°$

Although a weight torque arising from mass asymmetry can occur during the test of an ablating cone at zero incidence (due to an isolated turbulent wedge region, for example) the possibility of a weight torque contributing to the motion is more likely to occur when ablating wind-tunnel tests are made at finite angles of attack because uneven circumferential heating rates are involved. The effect of the weight torque (whether aiding or opposing the motion) will depend on the orientation of the model relative to the stream and the direction of spin. A movement of the c.g. location in the direction of the crossflow would be most noticeable for models tested in sideslip while the lateral component (relative to the crossflow) in c.g. travel would be most noticeable for models at angle of attack. In both cases, the direction of spin determines whether the weight torque has a damped or undamped effect on the roll rate. This suggests that dual, counter-rotating experiments should be conducted, both in pitch and yaw. Averages in the absolute values of the roll accelerations would be a reflection of aerodynamic values while differences would be related to weight torque contributions.

Other factors contributing to the roll motion are, as previously discussed, the internal torque of the gas bearing and residual effects of the model traversing the uneven heating environment of the tunnel boundary layer. However, these factors were relatively unimportant in the present investigation and did not affect the conclusions.

For the most meaningful experiment, in light of the above discussion of possible weight torque contributions, the program should involve test models initially spinning at both positive (counterclockwise) and negative (clockwise) roll rates in tests conducted at both positive and negative angles of attack and sideslip. Since the one Korotherm cone tested at angle of attack ($\alpha = -5°$) in the previous study[2] was prespun at about 8 rad/sec, the present tests were conducted to supplement the original test run. Initial roll rates of $p \approx 8$ rad/sec and $p \approx -8$ rad/sec were used and the models tested at $\alpha = +5°$ and $-5°$ (with $\beta = 0$) and at $\beta = +5°$ and $-5°$ (with $\alpha = 0$).

The test results for the eight ablating models are presented in Fig. 3 and the results for the metallic, nonablating models at $\alpha = 5°$ and $\beta = 5°$ are in Fig. 4. For the ablating test at $\alpha = -5°$ (Fig. 3a) the time required to insert the model into the stream was about 1 sec and the insertion process had a pronounced effect on the roll motion initially, with the effect persisting as a small oscillating motion superimposed on the general motion that clearly indicates a mean torque in the direction of spin for $2 < t < 17$. The remaining seven tests were made with the time to insert the model reduced to about $\frac{1}{2}$ sec, which noticeably decreased the starting transient effects.

For the nonablating models (Fig. 4) the results indicate

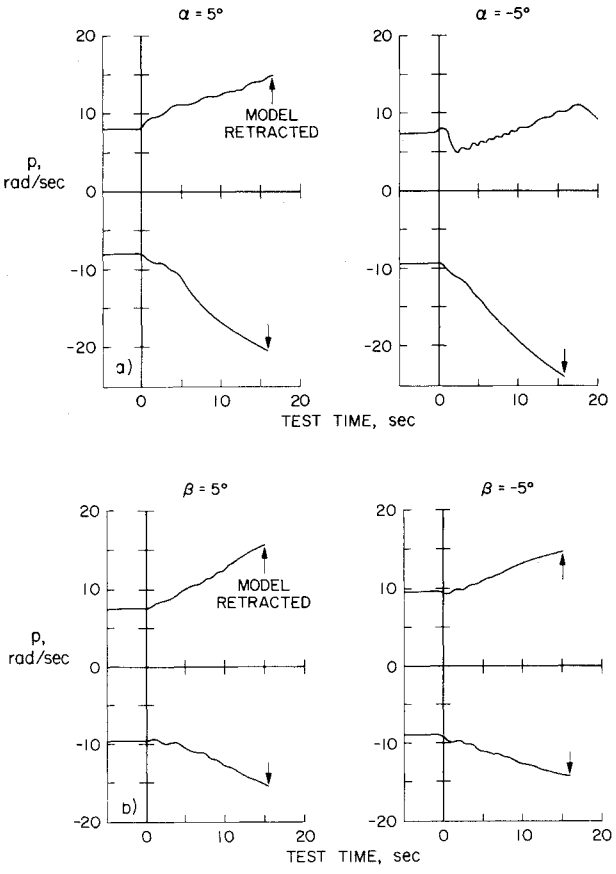


**Fig. 3 Roll characteristics of ablating models at angle of attack or sideslip; a) at angle of attack ($\beta = 0°$), b) at angle of sideslip ($\alpha = 0°$).**

aerodynamic damping approximately the same as for the zero-angle-attack case (Fig. 2a). For the ablating models (Fig. 3), however, all of the test results (ignoring the starting transient effects) indicate a torque in the direction of initial spin. The test times were limited to about 17 sec (except for the run at $\alpha = -5°$ included from Ref. 2), which ensured that the ablating surfaces remained smooth except for occasional indentations by dust particles in the stream and a transient liquid wave pattern at the start of each run, as previously discussed. Motion pictures of each test run, as well as inspection of the models after testing, verified that the ablating surfaces were essentially smooth and the spin-up torque evident in all of these tests could not be attributed to ablation striations. The effect of the internal torque of the gas bearing is negligible in the present experiments as is evident by the relatively small slopes of the data traces for $t < 0$. It is concluded, then, that the spin-up torques are the result of weight torques or aerodynamic torques induced by shape changes where the c.p. moves away from the roll axis.

A weight torque will aid the motion or damp the motion depending on the model orientation and the spin direction (see Fig. 5), whereas the direction of the aerodynamic torque will enter consistently as the product of (+ or −) (sign $p$), irrespective

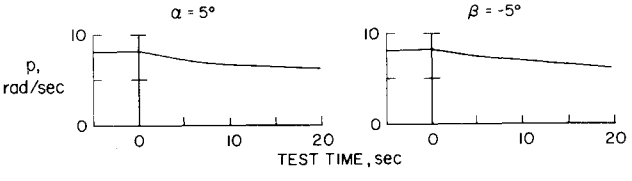


**Fig. 4 Roll characteristics of nonablating models at $\alpha = 5°$ and $\beta = -5°$.**

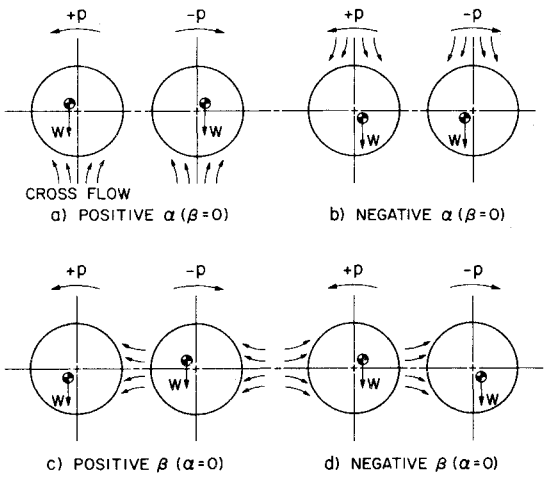


**Fig. 5 Spatial c.g. locations for spinning ablating cones at angle of attack or sideslip.**

of the orientation. If the weight-torque effect was to dominate, some of the models would spin up, some would spin down. However, the roll rate for all of the test models increased rapidly, indicating that the aerodynamic moment dominated for this experiment.

An attempt was made to evaluate the c.g. offsets, and resulting weight torques, by analyzing the results of Fig. 3 in accordance with the assumed behaviors shown in Fig. 5. Specifically, it was assumed that the roll torque is the sum of an aerodynamic moment due to friction forces, a tare moment (a known quantity), an aerodynamic moment due to pressure forces, and weight torques due either to lateral or vertical c.g. offsets. An appropriate set of relationships can then be expressed, using the test data, and solved simultaneously for the unknown moment contributions and c.g. offsets. It was found that the weight-torque contributions were small in comparison to the aerodynamic moments but could not be evaluated accurately because of the imprecise nature of the test results. The major differences in roll histories are attributed to inconsistent properties of cast Korotherm models that cure in somewhat different, individual manners.

The mean roll behavior of the eight test models, which should reflect only the aerodynamic rolling moment, is presented in Fig. 6. The roll acceleration ranged from about $|\dot{p}| = 0.4$ to about 1.3 rad/sec$^2$. For $\dot{p} = 0.5$ an applied torque of 3.2 g-cm (0.0028 lb-in.) is implied. Since the aerodynamic normal force on the model was 7.4 kg (16.2 lb) this torque would be obtained by a lateral movement in the model c.p. of only 0.00043 cm (0.00017 in.), which illustrates the extreme sensitivity of cones to ablation shape changes.

The probable cause for the spin-up of these smoothly ablating

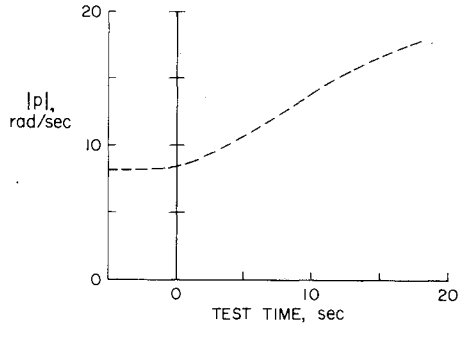


**Fig. 6 Summary of test results for the Korotherm models at $\alpha, \beta = \pm 5°$.**

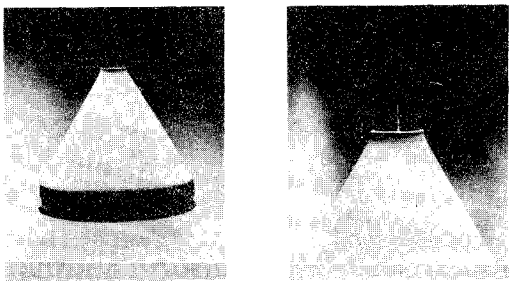


**Fig. 7 Postrun photographs of a 30° Korotherm cone.**

Korotherm models, rolling at small angles of attack, was concluded to be the thermal expansion properties of the ablating material, responding to the uneven circumferential heating introduced by angle of attack and spin. This phenomenon will be discussed next.

The test angles of attack and yaw ($\pm 5°$) were small in comparison to the cone angle (semivertex angle of 30°) and consequently neither flow separation nor vortex formations near the lee surfaces could be expected to be present or contribute to the roll motion. The possibility of friction forces introducing a spin-up torque was also ruled out since these forces are dissipative and invariably damp the motion whenever the motion itself does not alter the basic nature of the boundary layer or the basic nature of the flowfield (that is, neither flow separation, reattachment, nor hysteresis effects were present).

## Effect of Thermally Expanding Surfaces on Aerodynamic Roll Torque

A typical postrun photograph of an ablated Korotherm cone is shown in Fig. 7. Although about 15 g of the Korotherm was lost during 17 sec of ablation (the initial model weight was 510 g) the model size actually increased slightly because of thermal expansion in the thin ablating layer. The radius near the model base increased approximately 0.05 cm (0.02 in.). The unusually large thermal expansion immediately adjacent to the base of the metal tip (Fig. 7b) is the result of local postrun heating by the hot metal tip (motion pictures of the model during the test indicated smooth ablating surfaces with no apparent step at the base of the metal tip).

An explanation for the observed spin-up torque will be attempted on the basis of a first-order analysis of the effect of ablation shape changes on aerodynamic roll. To begin with, the spatial heating rate for a spinning cone at small angle of attack ($\alpha \ll \sigma_c$) is assumed to be of the form (see Fig. 8)

$$h = (x/l)^{-m}[h_0 + h_\alpha \alpha \cos(\theta - \varepsilon)] \tag{1}$$

where the coordinate system is fixed relative to the crossflow and the angle $\theta$ is measured from the most windward meridian. Spin (in the presence of angle of attack) shifts the point of maximum heating in the direction of spin, to $\theta = \varepsilon$, and it will be shown that it is this effect that is significant in causing aerodynamic roll torques when the thermal expansion characteristics of the ablator are appreciable. For zero spin and $m = \frac{1}{2}$, Eq. (1) has the form suggested by Moore's analysis[5,6] of the laminar boundary layer on cones at small angles of attack. The angle $\varepsilon$ is assumed to coincide with the location of the point of minimum boundary-layer thickness, and Sedney's analysis[7] (see also Ref. 8) shows this angle to be proportional to the local surface roll velocity

$$\varepsilon \sim pr/U_e$$

or

$$\varepsilon = K_\varepsilon (x/l)(\tan \sigma_c) p \tag{2}$$

where $K_\varepsilon$ is a positive parameter with dependence on cone angle and stream environment.

Next, a constant roll rate is assumed and thermal lag in the material response is neglected. The change in spatial body radius is assumed to be the result of mass removal and material expansion, both varying with the heating-rate input. The change in body radius due to mass removal may be expressed as

$$(R-r)_1 = -\lambda_1 h^{\bar{n}_1} \tag{3}$$

and the change due to thermal expansion as

$$(R-r)_2 = \lambda_2 h^{\bar{n}_2} \tag{4}$$

where $r$ is the initial body radius. Since it has been assumed that $\alpha \ll \sigma_c$ the ratio $h_\alpha/h_0$ [see Eq. (1)] is less than unity, and the shape change due to mass removal is approximately

$$\begin{aligned}(R-r)_1 &\approx -\lambda_1 (x/l)^{-n_1} h_0^{\bar{n}_1}[1 + \bar{n}_1 (h_\alpha/h_0)\alpha \cos(\theta - \varepsilon)] \\ &\approx -(x/l)^{-n_1}[\Delta r_1 + K_1 \alpha \cos(\theta - \varepsilon)]\end{aligned}$$

The thermal expansion effect can be expressed in a similar fashion. Thus the appropriate expression for body shape change is

$$\begin{aligned}R - r = &-(x/l)^{-n_1}[\Delta r_1 + K_1 \alpha \cos(\theta - \varepsilon)] + \\ &(x/l)^{-n_2}[\Delta r_2 + K_2 \alpha \cos(\theta - \varepsilon)]\end{aligned} \tag{5}$$

where subscripts 1 refer to the mass removal effect, subscripts 2 refer to the thermal expansion effect, and the parameters $\Delta r_{1,2}, K_{1,2}$ take on positive values only by definition.

If the pressure coefficient is estimated by Newtonian theory (the effect of the boundary-layer displacement thickness on pressure is neglected in this first-order analysis), the aerodynamic roll torque about the cone axis, arising from the shape change described by Eq. (5), is

$$\begin{aligned}C_l = \frac{\alpha \cot^2 \sigma_c}{2\pi} &\int_0^1 [K_1 (x/l)^{1-n_1} - K_2 (x/l)^{1-n_2}]\, d(x/l) \times \\ &\int_0^{2\pi} C_p \sin(\theta - \varepsilon)\, d\theta \\ = 2 \cot \sigma_c &[K_2 (3-n_2)^{-1} - K_1 (3-n_1)^{-1}] \alpha (\sin \varepsilon_b) \times \\ &(\cos^2 \sigma_c)(\sin \alpha) \cos \alpha\end{aligned}$$

If the normal force is approximated by (Newtonian)

$$C_N = 2(\cos^2 \sigma_c) \sin \alpha \cos \alpha$$

the roll torque about the cone axis may be expressed as

$$C_l = \cot \sigma_c (\bar{K}_2 - \bar{K}_1) \alpha C_N \sin \varepsilon_b \tag{6}$$

where

$$\bar{K}_1 = K_1/(3-n_1), \quad \bar{K}_2 = K_2/(3-n_2) \tag{7}$$

Since $\sin \varepsilon_b \approx \varepsilon_b = K_\varepsilon (\tan \sigma_c) p$ and $C_N$ may be approximated for small $\alpha$ as $C_N = C_{N_\alpha} \alpha$, the roll torque may also be expressed as

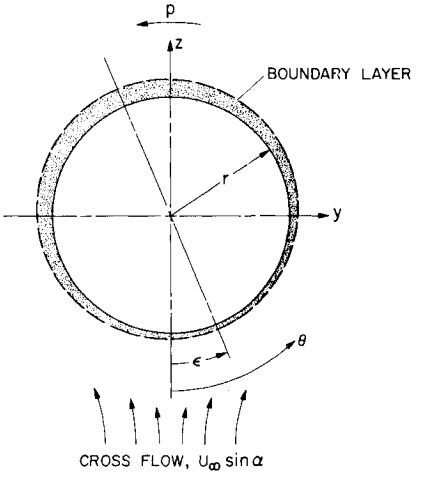


**Fig. 8 Nomenclature (base view of cone at angle of attack).**

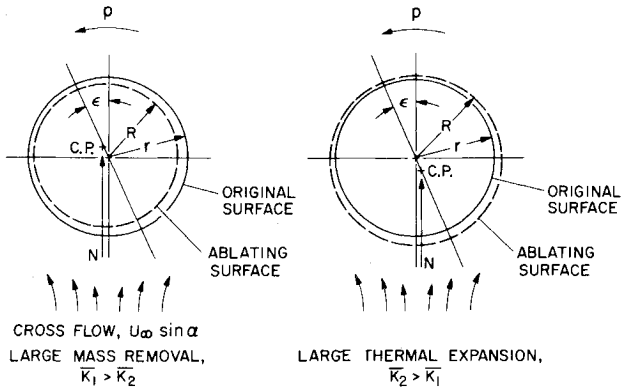


**Fig. 9 Shape changes and lateral position of c.p. for rolling models at angle of attack in the wind tunnel.**

$$C_l = [K_c C_{N_\alpha} \alpha^2](\bar{K}_2 - \bar{K}_1)p \tag{8}$$

The bracketed quantity above is always positive and thus the torque has the sign of $(\bar{K}_2 - \bar{K}_1)p$.

When the shape changes due to thermal expansion are much greater than changes due to mass removal [i.e., $(\ )_2 > (\ )_1$ in Eq. (5)] the resulting aerodynamic roll torque is in the direction of spin. This was the case for the Korotherm models tested in the present investigation. The spin-up behavior is to be expected on the basis of the above analysis. If, however, the body decreases in size [i.e., $(\ )_1 > (\ )_2$ in Eq. (5)] the roll torque is opposite the direction of spin and the motion is damped. The two cases just described are shown in Fig. 9.

For the wind-tunnel tests the motion is constrained to rotation about the original cone axis whereas in the flight case the motion is about the instantaneous mass center. Thus it is informative to consider the location of shape changes described by Eq. (5) on c.g. location and to compare the wind-tunnel case with flight case. First of all, the thermal expansion effect is to redistribute, radially, the mass in the thermal ablation layer but it can be shown that the effect on c.g. location is second-order in $\Delta r/r$. Thus the quantities $(\ )_2$ in Eq. (5) do not affect the mass center (to first-order).

When the mass removal effect is considered (finite $K_1$) the spatial c.g. coordinates are, of course, affected. In evaluating the effects of shape changes on roll torque for the flight case it will be assumed that the specific gravity of the ablator is equal to the average density of the vehicle. If the ablator density differs slightly from the average density, the effect on roll torque appears in a second-order term when mass is removed so inclusion in the present first-order analysis would be inappropriate. Assuming, then, a homogeneous cone the rolling moment is

$$C_{l_{c.g.}} = (A_b d)^{-1} \int_0^l dx \int_0^{2\pi} [C_p R(\partial R/\partial\theta) - \bar{y} C_p R \cos\theta]\, d\theta$$

where

$$\bar{y} \approx (1/\pi) \int_0^{2\pi} R^3 (3r^2)^{-1} \sin\theta\, d\theta$$

Considering only first-order terms gives

$$C_{l_{c.g.}} = K_c C_{N_\alpha} \alpha^2 \bar{K}_2 p \tag{9}$$

Note that this result is independent of $K_1$ (the mass removal effect does not contribute to the roll torque in the flight case). The effects of shape changes on mass center and c.p. for rolling models at angle of attack in free flight are illustrated in Fig. 10.

The effect of shape changes on roll torque for the wind-tunnel model is given by Eq. (8) and for the flight model by Eq. (9). The aerodynamic skin-friction forces should contribute a damping moment in both cases, and if this moment is approximated by

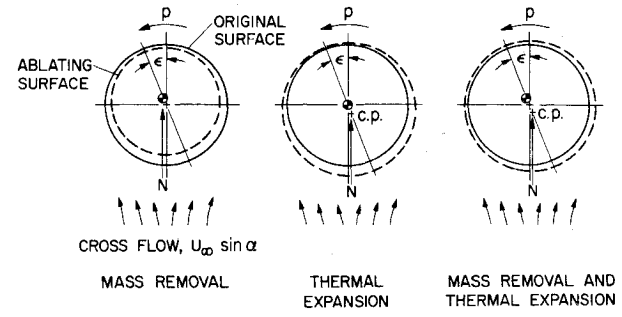


**Fig. 10 Shape changes and lateral positions of mass center and c.p. for rolling models at angle of attack in free flight.**

$$C_{l_f} = C'_{l_f} p$$

the aerodynamic roll torque for rolling models at angle of attack may be summarized as follows:

for the wind-tunnel model

$$C_l = K_c C_{N_\alpha} \alpha^2 (\bar{K}_2 - \bar{K}_1)p - C'_{l_f} p \tag{10}$$

for the flight model

$$C_l = K_c C_{N_\alpha} \alpha^2 \bar{K}_2 p - C'_{l_f} p \tag{11}$$

The mass removal parameter $\bar{K}_1$ does not enter the flight case. If the thermal expansion is large so that $\bar{K}_2 > \bar{K}_1$ the shape-change torque is larger for the flight case, in comparison with the wind-tunnel case, by the ratio $\bar{K}_2/(\bar{K}_2 - \bar{K}_1)$. Whether spin-up occurs, however, depends on the relative importance of the skin-friction damping.

## Concluding Remarks

Previous wind-tunnel studies have shown that aerodynamic torques can arise when ablation surface patterns of various kinds appear. This study has shown that the smoothly ablating cone, rolling at angle of attack or sideslip, can also experience unstable aerodynamic roll torques if the thermal expansion properties of the ablator are sufficiently large.

An analysis of the effects of two smooth ablation shape changes (mass removal and thermal expansion) on the roll motion at angle of attack was included in the study. For the wind-tunnel test model (motion constrained to rotation about the cone axis) the effect of mass removal is to damp the motion but the effect of surface thermal expansion is to introduce a torque in the direction of spin. If the thermal expansion effect dominates (which was the case for the Korotherm models tested), a spin-up torque results. For the flight case (motion about the instantaneous mass center) the effect of mass removal is negligible (unless the specific density of the ablator differs appreciably from the average density of the vehicle, a second-order contribution not included in the present analysis). The effect of surface thermal expansion in the flight case is to also introduce a torque in the direction of spin and the magnitude could be expected to be larger than that experienced by the wind-tunnel model in a similar environment.

It should be emphasized that, in order to estimate the magnitude of the roll torque arising from thermal expansion of an ablating surface, a precise knowledge of the thermal expansion characteristics at ablation temperatures is necessary (particularly if a melt layer is involved) and thus the characteristics at temperatures below the ablation level would probably not be meaningful in most cases.

## References

[1] Williams, E. P., "Experimental Studies of Ablation Surface Patterns and Resulting Roll Torques," *AIAA Journal*, Vol. 9, No. 7, July 1971, pp. 1315–1321.

[2] McDevitt, J. B., "An Exploratory Study of the Roll Behavior of

Ablating Cones," *Journal of Spacecraft and Rockets*, Vol. 8, No. 2, Feb. 1971, pp. 161–169.

[3] Nachtsheim, P. R., "Analysis of the Stability of a Thin Liquid Film Adjacent to a High-Speed Gas Stream," TN D-4976, 1969, NASA.

[4] Nachtsheim, P. R. and Hagen, J. R., "Observations of Crosshatched Wave Patterns in Liquid Films," AIAA Paper 71-622, Palo Alto, Calif., 1971.

[5] Moore, F. K., "Laminar Boundary Layer on a Circular Cone in Supersonic Flow at a Small Angle of Attack," TN 2521, 1951, NACA.

[6] Moore, F. K., "Displacement Effect of a Three-Dimensional Boundary Layer," TN 2722, 1952, NACA.

[7] Sedney, R., "Laminar Boundary Layer on a Spinning Cone at Small Angle of Attack in a Supersonic Flow," *Journal of the Aeronautical Sciences*, Vol. 24, No. 6, June 1957, pp. 430–436.

[8] Martin, J. C., "On Magnus Effects Caused by the Boundary-Layer Displacement Thickness on Bodies of Revolution at Small Angles of Attack," *Journal of the Aeronautical Sciences*, Vol. 24, No. 6, June 1957, pp. 421–429.

APRIL 1973 AIAA JOURNAL VOL. 11, NO. 4

# Ballistic Range Investigation of Sonic-Boom Overpressures in Water

PETER F. INTRIERI* AND GERALD N. MALCOLM†
*NASA Ames Research Center, Moffett Field, Calif.*

**An investigation of sonic-boom overpressures in water has been conducted in the Ames Research Center Pressurized Ballistic Range by gun-launching small cone-cylinder models over water. Flights were conducted at Mach numbers of 2.7 and 5.7 in air, corresponding to Mach numbers of 0.6 and 1.3, respectively, in water. Shadowgraph pictures and underwater pressure measurements indicate that for horizontal flights at Mach numbers below Mach 4.4 in air (i.e., subsonic Mach numbers relative to the speed of sound in water) the resulting underwater disturbance is an acoustic wave whose peak pressure attenuates rapidly with water depth. Comparison of experimental data for the subsonic case with existing theoretical predictions of attenuation with depth shows good agreement. In contrast, at supersonic Mach numbers, relative to water, the incident shock wave at the surface is transmitted into the water as a propagating shock wave and the peak pressure associated with it is not affected by water depth but attenuates as it does in air.**

## Nomenclature

$a$ = speed of sound
$h$ = distance from flight path to pressure cell
$h_w$ = distance from flight path to water surface
$l$ = model reference length
$M$ = Mach number
$\Delta p$ = overpressure or pressure change from ambient pressure
$\Delta p_o$ = overpressure at water surface behind reflected incident shock wave
$\Delta p_{max}$ = maximum or peak overpressure from ambient pressure
$t$ = time
$T$ = period of N-wave
$V$ = velocity of incident shock wave in air parallel to water surface (also velocity of model in flight)
$\zeta$ = normalized depth parameter [see Eq. (1)]
$\theta$ = angle of incidence between incident shock wave and water surface
$\theta_c$ = critical angle of incidence
$\mu$ = Mach angle, $\sin^{-1} 1/M$
$\tau$ = normalized time parameter, $t/T$

Presented as Paper 72-657 at the AIAA 5th Fluid and Plasma Dynamics Conference, Boston, Mass., June 26–28, 1972; submitted July 2, 1972; revision received November 15, 1972. The authors thank R. Hicks and J. Mendoza of Ames Research Center for bringing to our attention the apparent need for underwater sonic boom tests, and M. Wilkins, for his assistance in obtaining the shadowgraph pictures and performing the fish experiments.

Index categories: Aerodynamic and Powerplant Noise (Including Sonic Boom); Atmospheric, Space, and Oceanographic Sciences; Undersea Acoustics.

* Research Scientist.

† Research Scientist. Member AIAA.

## Introduction

THERE is a great deal of concern about the effects of sonic-boom overpressures over land and populated areas. There has been less concern about overpressures that occur over water and the resulting underwater pressure disturbances. It is important to understand these disturbances since they may have significant underwater environmental effects. To date, a few theoretical and experimental studies concerning underwater pressures induced by sonic booms have been conducted. Sawyers[1] and Cook,[2] for example, have developed similar theories for the case of a planar N-wave traveling horizontally over a smooth water surface at a constant speed less than the speed of sound in water ($M_{air} < 4.4$). Their results indicate that the incident shock wave at the air-water interface is totally reflected and the pressure disturbance at the surface penetrates into the water as sound waves. Furthermore, the sound pressure is shown to attenuate rapidly with both increasing frequency and depth in the water. To test the validity of these theories, Waters and Glass[3] conducted experiments using air blasts from explosive charges over a water surface (flooded quarry, 90 m wide and 24 m deep) to produce shock waves simulating a sonic boom. Pressure measurements were made underwater at various depths and their results showed good agreement with Sawyers' theory.[1] Conversely, Urich,[4] using minimal data obtained from a few aircraft flights over the ocean and hydrophones submerged at various depths, concludes that peak pressures fall off more rapidly with depth than predicted and therefore the existing theories are not valid. The only explanation offered for the discrepancy was a possible effect from wave scattering due to a rough sea surface. Thus, from the literature, it appears that additional work concerning sonic-boom effects underwater is warranted even for the